

Estimation of the maximum end buffer impact force for a given level of reliability

T N Haas, P Mainçon, P E Dunaiski

The first paper in this set of two, titled *The effect of parameters on the end buffer impact force history of the crane* (see page 55), examined the effect of a change in the magnitude of the parameter on the end buffer impact force history. This paper investigates to what degree a change in the magnitude of the parameter alters the impact force history. This was accomplished through a sensitivity analysis performed by individually varying the magnitude of the parameter in the FE model. For each case individual maximum impact forces were obtained. The maximum impact force could not simply be selected by choosing the greatest value from the sensitivity study. A constraint optimisation technique for a given level of reliability (β) using the FE simulation data was used to determine the maximum impact force. A comparison between the constraint optimisation and codified results showed that SABS 0160-1989 underestimates the impact force by 18%, while SANS 10160-2010 substantially overestimates the impact force by 64% for a level of reliability of $\beta = 3$. If the relevant clauses of SANS 10160-6 that pertain to end stop design are used in their present form, this will result in a conservative design, whereas SABS 0160 has a probability of 2.3% of being exceeded.

INTRODUCTION

Underestimation of the end buffer impact forces as a result of a collision between the crane and the supporting structure can lead to disastrous consequences. This could result in the crane running off the rails during impact if the end stops fail. Although the cost of increasing the end stop connections is minimal compared to the overall cost of the structure, the cost of failure if the crane ran off the crane rails would be significant and could lead to fatalities. Some structural engineering professionals who were consulted increase the impact force because they are uncertain whether the codified estimations would prevent a major catastrophe. The guidelines and design codes considered in this study are:

- South African Standard: SABS 0160 – 1989 (as amended 1990)
- Manufacturer's guidelines: DEMAG
- Eurocode 1, Part 3, EN 1991
- South African National Standard: SANS 10160 – Part 6
- Australian Standard: AS 1418.14 – 2001
- Australian Standard, AS 1418.1 – 1994
- Association of Steel and Iron Engineer's technical report, AISE No 13 – 1997

The design codes of practice use various approaches to estimate the impact force as described in the accompanying paper on page 55. Table 1 of the accompanying paper shows the limited number of parameters which the design codes take into account to

estimate the impact force. These approaches are followed to simplify the calculations. Also, all the design codes consider the crane and the supporting structure as a decoupled system to estimate the impact force. This can lead to significant errors in the estimation of the impact force.

In the accompanying paper, evidence was provided that the parameters do have an effect on the impact force histories. This paper describes a sensitivity study conducted to determine the influence of individual parameters on the end buffer impact force history. From this information the maximum impact force was determined for a given level of reliability using a constraint optimisation technique.

This paper also determined whether the design codes yield reasonable impact force estimates when compared to the constraint optimisation results for a given level of reliability (β). The results of this study provide a tool which structural engineering professionals can use to assess the codified end buffer impact force results.

Several papers have been published on the control mechanism to prevent the hoist load from oscillating during longitudinal travel. However, apart from the design codes, no papers were found in which the impact force is directly estimated when the crane collides with the end stops.

The sections below examine the methods used in the sensitivity study – only the



DR TREVOR HAAS (Pr Tech Eng) is a Senior Lecturer in Structural Engineering at the Stellenbosch University. He obtained the National Diploma (1991) and National Higher Diploma (1992) in Civil Engineering from the former Peninsula Technikon, now Cape Peninsula University of Technology. In 1999 he was awarded the MSc in Civil Engineering from

Southern Illinois University at Carbondale, USA. In 2007 he was awarded a PhD from the University of Stellenbosch. His research interests include numerical (FEA) modelling of steel structures, retrofitting of existing structures, structural dynamics and engineering education. He is a member of the Engineering Council of South Africa's universities of technology accreditation team.

Contact details:

Stellenbosch University
Department of Civil Engineering
Private Bag X1
Matieland
7602
South Africa
T: +27 21 808 4438
E: trevor@sun.ac.za



DR PHILIPPE MAINÇON obtained his engineering degree from the Ecole Centrale de Paris (France) and his Dr Ing degree from the Norwegian University of Science and Technology (Norway). He has lectured numerical methods in structural engineering at the University of Stellenbosch (South Africa), and is currently working at Marintek (Norway) as

a Senior Scientist. His research interests include inverse finite element methods for the processing of measurement data, flexible pipelines and risers for offshore applications, and vortex induced vibrations.

Contact details:

MARINTEK
SINTEF Marine
Otto Nielsens veg 10
Trondheim
Norway
T: +47 73 59 5687
E: Philippe.Maincon@marintek.sintef.no



PROF PETER DUNAISKI (Pr Eng), who sadly passed away in September 2011, was Professor in Structural Engineering at the University of Stellenbosch. He obtained the HBEng (1974), the MEng (1984) and the PhD (1991) degrees from the same university. His research interests were experimental mechanics and steel construction, with a focus on design aspects of commercial and industrial structures. At the time of the preparation of this paper, he was also involved in code development for the South African structural engineering practice.

Keywords: crane, impact force, constraint optimisation

Table 1 Parameters identified for the FE sensitivity analysis which could have a significant effect on the impact history

Parameter (Variable)	Base Value	Range of Variation	Interval of Variation
Lag of the centre of gravity (COG) of the hoist load with respect to the crane bridge	0°	2.50° ±	1.25° ± 2.50° ±
Crab and hoist load eccentricity on the crane bridge	0 m	3.39 m ±	1.695 m ± 3.390 m ±
End stop misalignment	0	150 mm	25 mm 50 mm 150 mm
Flexibility of the crane supporting structure	Rigid ≈ 0	Weak, intermediate and strong spring	Spring stiffness varied
Crane velocity on impact	0.55 m/s	– 0.165 m/s	0.05 m/s ± – 0.165 m/s
Elastic characteristics of buffer	Stiffness curve used in FEA	20% ±	10% ± 20% ±
Damping characteristics of buffer	Damping used in FEA	Without damping	Without damping

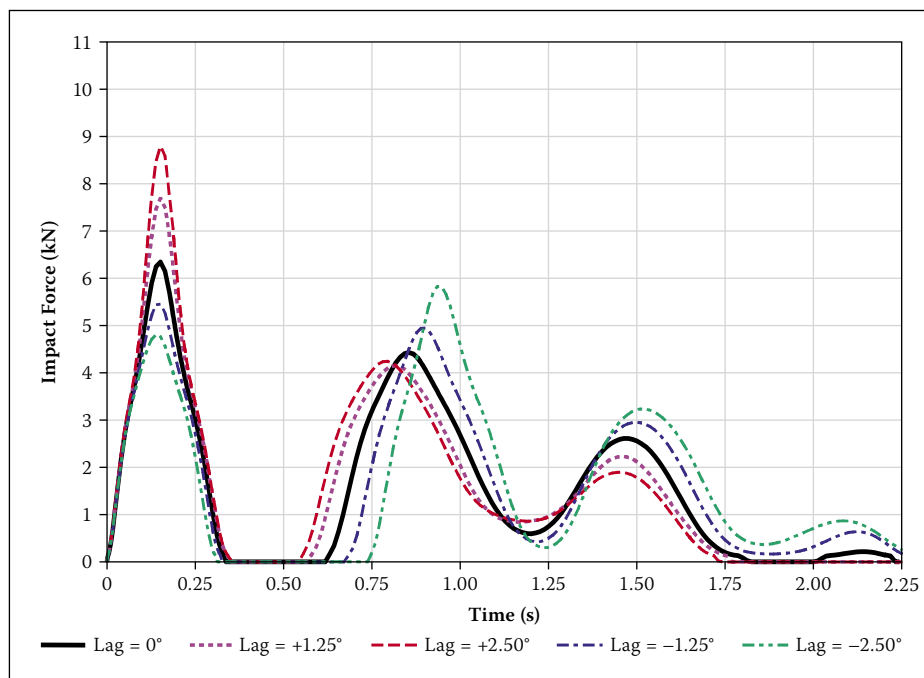


Figure 1 Impact force: hoist load bottom with “Power-Off” for the hoist load lag

horizontal lag of the hoist load is reviewed and discussed; the maximum end buffer impact force is estimated, which includes the probability of the parameters, the design point and the probability of exceedance, and the results of the constraint optimisation technique are given. The paper ends with a conclusions section.

METHODS USED IN THE SENSITIVITY STUDY

The impact force histories shown in Figure 9 of the accompanying paper were obtained without a detailed sensitivity analysis. They were obtained by simply choosing a reasonable variation of the magnitude of the parameter for the FE simulations. In the

present paper, the FE model described in the accompanying paper and the variation of the magnitude of the parameters were used to conduct a detailed sensitivity analysis. The range of variation of the parameters was obtained by carefully examining the video footage of the experimental tests and the FE simulations. Table 1 shows the parameters with their corresponding base state, range of variation and interval of variation.

The impact force history was obtained by varying the magnitude of a single parameter while keeping the remaining parameters constant. This approach allowed the impact force history of the individual parameter’s mode of vibration to be obtained, i.e. the response of only one parameter on the impact force history. Besides adjusting the

magnitude of the parameters, FE simulations were also conducted for the following cases:

1. “Power-Off hoist load bottom”, i.e. the impact occurred as a result of the crane’s inertia when the hoist load was raised 0.15 m above ground level.
2. “Power-On hoist load bottom”, i.e. during impact the longitudinal motors were constantly engaged with the hoist load raised 0.15 m above ground level.
3. “Power-Off hoist load top”, i.e. the impact occurred as a result of the crane’s inertia when the hoist load was raised 2.20 m above ground level.
4. “Power-On hoist load top”, i.e. during impact the longitudinal motors were constantly engaged with the hoist load raised 2.20 m above ground level.

Due to limited space and to prevent repetition, only one parameter, i.e. the horizontal lag angle of the hoist load, is discussed in detail.

REVIEW OF PARAMETER: HORIZONTAL LAG OF THE HOIST LOAD

Impact force history: Parameter = horizontal lag of the hoist load

This parameter was investigated as all the codes of practice, except for SANS 10160-6 and EN 1991:3–2003, ignore the effect of the hoist load if it is not rigidly restrained (fixed) to the crane bridge. To study the horizontal lag effect of the hoist load on the impact force history, the cable and hoist load were inclined at angles of 1.25° ± and 2.50° ± from the vertical at the moment of impact. A positive lag is defined as the hoist load ahead of the crane bridge at the moment of impact.

Results of the sensitivity study of the horizontal lag of the hoist load

The effect of the hoist load lag on the impact force history is shown in Figures 1 and 2 when the hoist load is raised 0.15 m and 2.20 m above ground level for the “Power-Off” conditions.

Sensitivity study of the horizontal lag of the hoist load

The following information was extracted from Figures 1 and 2 for the horizontal lag of the hoist load:

Case: hoist load bottom

- A positive increase in the lag angle resulted in a substantial increase in the magnitude of the first impact force, while the magnitude of the second impact force was only marginally affected.

- The opposite occurred for a negative lag angle, except that the second impact force increased proportionately as the negative lag angle increased.
- The position of the first impact peak was insignificantly affected, while a significant positive shift of the second peak was observed for a negative lag angle, and a significant negative shift was observed for a positive lag angle.

Case: hoist load top

The impact force history for the hoist load top case follows a similar trend as for the hoist load bottom case, except that the magnitudes and position of the second impact force were insignificantly affected.

SUMMARY OF THE FE SIMULATIONS

The sensitivity study of the remaining parameters showed similar trends. Refer to Haas (2007) for a complete review of the effect of a change in magnitude of the remaining parameters.

Table 2 presents the significant information that was extracted from the FE simulations when the peak forces were compared to the base states for six of the seven parameters listed in Table 1. The remaining parameter, the elastic characteristics of the buffer, was disregarded due to its insignificant effect on the end buffer impact force histories. It is important to note that, although the impact histories are

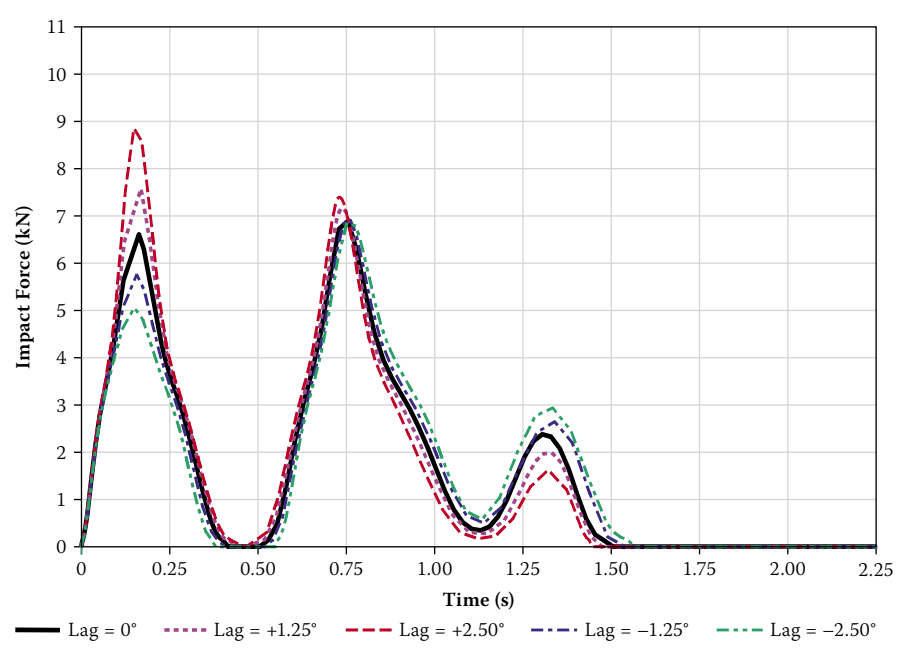


Figure 2 Impact force: hoist load top with "Power-Off" for the hoist load lag

not significantly affected, the displacement histories show a moderate change.

When the magnitude of the parameter was varied, it could yield either a positive or negative change in the first and second impact peaks, as well as a position shift of the impacts. This is clearly illustrated in Figures 1 and 2 for a variation of the lag angle of the hoist load. From Table 2, the maximum percentage positive increase for the first peak when the hoist load was raised 0.15 m and 2.20 m above ground level

was 38% and 37% respectively. For the second peak, the maximum percentage positive increase was 211% and 57%. The maximum time difference between the peaks was 32% and 34% respectively when the hoist load was raised 0.15 m and 2.20 m above ground level.

Impact force histories for arbitrarily selected parameters

Figure 3 shows the impact force histories of arbitrarily selected simulations for six of the

Table 2 Summary of significant information obtained from the FE simulations

Parameter	Hoist Load Position for "Power-Off" and "Power-On"	First Peak Magnitude		Second Peak Magnitude		Time Between Peaks	
		Maximum % Positive Increase	Maximum % Negative Decrease	Maximum % Positive Increase	Maximum % Negative Decrease	Maximum % Positive Difference in Position	Maximum % Negative Difference in Position
Hoist Load Lag	Bottom	+ 38	- 26	+ 32	- 6	+ 14	- 10
	Top	+ 33	- 25	+ 7	- 11	+ 3	- 3
Hoist Load and Crab Eccentricity	Bottom	+ 22	N/A	+ 31	N/A	0	- 4
	Top	+ 26	N/A	+ 18	N/A	5	- 2
Flexibility of the Crane Supporting Structure	Bottom	+ 5	- 31	+ 49	- 1	+12	- 3
	Top	0	- 34	+ 14	- 10	+ 34	- 2
Impact Velocity of the Crane	Bottom	+ 24	- 46	+ 53	- 41	+ 1	- 9
	Top	+ 25	- 51	+ 28	- 54	+ 2	- 3
End Stop Misalignment	Bottom	+ 33	N/A	+ 65	N/A	+ 32	N/A
	Top	+ 37	N/A	+ 37	- 15	+ 34	N/A
Damping Characteristics of the Buffer	Bottom	+ 20	N/A	+ 211	N/A	+ 17	N/A
	Top	+ 20	N/A	+ 57	N/A	+ 10	N/A
Maximum Percentage Difference	Bottom	+ 38	- 46	+ 211	- 41	+ 32	- 10
	Top	+ 37	- 51	+ 57	- 54	+ 34	- 3

Note: N/A means that the first and second impact forces were greater than the base state, and thus no impact forces lower than the base state were obtained.

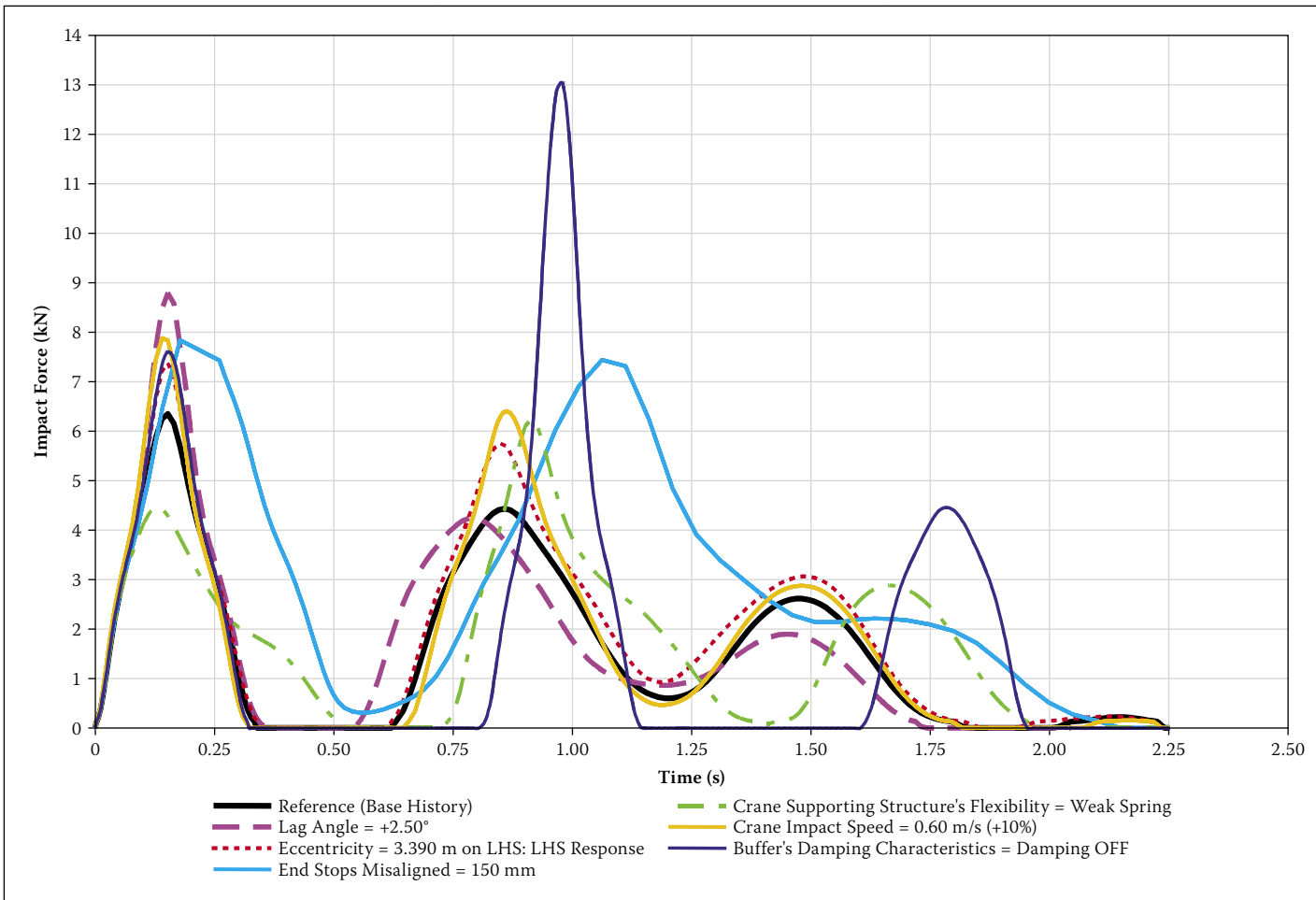


Figure 3 Selected impact force response of each parameter compared to base response when hoist load is raised to 0.15 m above ground level

Table 3 Change in force per parameter when the impact forces are 3σ from the base value for the first impact response

Parameter	Hoist Load Bottom "Power-Off"	Hoist Load Bottom "Power-On"	Hoist Load Top "Power-Off"	Hoist Load Top "Power-On"
	Change in Force (kN)	Change in Force (kN)	Change in Force (kN)	Change in Force (kN)
Base Impact Force (f_O)	6.35	7.26	6.65	7.48
1. Lag Angle	3.17	3.69	2.50	3.56
2. Crab and Hoist Load Eccentricity	1.08	1.52	1.53	2.03
3. Flexibility of Crane Supporting Structure	-2.66	-3.06	-2.63	-1.52
4. Crane Impact Speed	4.13	4.73	4.43	4.88
5. One End Stop Misaligned	3.69	4.17	4.85	5.19
6. Damping Characteristics of Buffer	1.13	1.31	1.21	1.38

seven parameters investigated when the hoist load was raised to 0.15 m above ground level.

The results from Figure 3 confirm that the individual parameters do have a substantial influence on the impact force histories in terms of magnitude and position. Improved agreement with the experimental impact force histories could be obtained by adjusting the magnitude of the parameters. However, the magnitude of the adjusted parameters will only be valid for the specific case, as the

impact force history is very sensitive to the variation of the individual parameters.

ESTIMATION OF THE MAXIMUM END BUFFER IMPACT FORCE

The end buffers must be designed to have some arbitrarily chosen, low probability of failure if an impact occurs. Thus the question arises as to what impact force the end buffers must be designed to withstand. A more convenient way to address the same question is to

ask: for a given end buffer capacity (f_c), what is the probability of failure under impact?

Linear load model

The FE analysis provided information on the effect of various parameters on the impact force. Since only one parameter was varied at a time and only in one increment, only the *gradient* of the impact force could be assessed, which led to the choice of a *linear* model. Clearly this assumption of linearity is a weak link in the present work. Reinforcing the link would require a much wider set of FE analyses to be carried out.

The linear model is of the form:

$$f(\bar{\Delta P}) = f(0) + \sum_{i=1}^n \frac{\partial f}{\partial P_i} \cdot \Delta P_i \\ = f(0) + (\bar{\nabla}_P f)^T \cdot \bar{\Delta P} \quad (1)$$

where:

$f(\bar{\Delta P})$ is the end buffer impact force, $\bar{\Delta P} = \bar{P} - \bar{P}_0$ is the change in the parameters where \bar{P}_0 is the nominal value of the parameters (at which the gradient was assessed), n is the number of parameters.

The changes in force $\left(\frac{\partial f}{\partial P_i} \cdot \Delta P_i \right)$ for each parameter for all four cases studied using

FE, i.e. Hoist load bottom “Power-Off”, Hoist load bottom “Power-On”, Hoist load top “Power-Off” and Hoist load top “Power-On” for $\Delta P_i = 3\sigma_i$ (a change in parameter of three standard deviations), are presented in Table 3 for the first impact and in Table 4 for the second impact.

Probability distribution of the parameters

A probability density can be associated to any value of $\bar{\Delta P}$. Since only information on standard deviation is available, a reasonable model to use was a multinomial Gaussian distribution:

$$p(\bar{\Delta P}) = (2\pi)^{-n/2} \det(\bar{C})^{1/2} \exp(-\frac{1}{2} \bar{\Delta P}^T \cdot \bar{C}^{-1} \cdot \bar{\Delta P}) \quad (2)$$

where:

\bar{C} is the covariance matrix.

Since no cross-correlation information was available, \bar{C} was taken as diagonal, with the square of the deviation of each parameter on the diagonal. The standard deviations of each parameter presented in Table 5 were obtained from engineering judgement and a review of video footage of the experimental tests and FE simulations.

Design point

Finding the combination of parameters leading to a given load with the highest value of $p(\bar{\Delta P})$ is equivalent to finding the combination of parameters leading to the same load, with the lowest value of

$$g(\bar{\Delta P}) = -\frac{1}{2} \bar{\Delta P}^T \cdot \bar{C}^{-1} \cdot \bar{\Delta P} \quad (3)$$

Hence this leads to Equation 4 which must be solved.

Find $\bar{\Delta P}$ that minimises

$$g(\bar{\Delta P}) = -\frac{1}{2} \bar{\Delta P}^T \cdot \bar{C}^{-1} \cdot \bar{\Delta P} \quad (4)$$

under the constraint

$$f_c = f(0) + (\bar{\nabla}_P f)^T \cdot \bar{\Delta P}$$

This is a *constrained minimisation problem*. One convenient way to solve this is to transform Equation 4 into an unconstrained minimisation problem by means of Lagrange multipliers which can show that the above problem is equivalent (Larson 1995) to solving

Find $\bar{\Delta P}$ and λ for which

$$g^*(\bar{\Delta P}) = \frac{1}{2} \bar{\Delta P}^T \cdot \bar{C}^{-1} \cdot \bar{\Delta P} + \lambda((\bar{\nabla}_P f)^T \cdot \bar{\Delta P} + f(0) - f_c) \text{ is extremal} \quad (5)$$

This again can be shown that it amounts to solving the linear system of equations:

Table 4 Change in force per parameter when the impact forces are 3σ from the base value for the second impact response

Parameter	Hoist Load Bottom “Power-Off”	Hoist Load Bottom “Power-On”	Hoist Load Top “Power-Off”	Hoist Load Top “Power-On”
	Change in Force (kN)	Change in Force (kN)	Change in Force (kN)	Change in Force (kN)
Base Impact Force (f_O)	4.43	4.61	6.88	8.05
1. Lag Angle	-1.19	-0.96	0.38	1.09
2. Crab and Hoist Load Eccentricity	0.72	1.43	1.73	1.28
3. Flexibility of Crane Supporting Structure	-1.48	-1.61	-2.96	-3.04
4. Crane Impact Speed	4.16	5.03	4.43	6.26
5. One End Stop Misaligned	2.46	4.75	3.39	2.58
6. Damping Characteristics of Buffer	7.74	8.75	3.50	3.99

Table 5 Estimated standard deviation for each parameter

Parameter	Estimated Standard Deviation (σ)
1. Lag Angle	0.022 Radians (1.25°)
2. Crab and Hoist Load Eccentricity	1.13 m
3. Flexibility of Crane Supporting Structure	0.0025 m (2.5 mm)
4. Crane Impact Velocity	0.05 m/s
5. One (1) End Stop Misaligned	0.04125 m (41.25 mm)
6. Elastic Characteristics of Buffer	20%
7. Damping Characteristics of Buffer	30%

Table 6 Estimated maximum end buffer impact force from the first impact response

	Hoist Load Bottom “Power-Off”	Hoist Load Bottom “Power-On”	Hoist Load Top “Power-Off”	Hoist Load Top “Power-On”
Estimated maximum end buffer impact force for $\beta = 1$	7.64	9.05	8.44	9.83
Estimated maximum end buffer impact force for $\beta = 2$	8.93	10.83	10.23	12.19
Estimated maximum end buffer impact force for $\beta = 3$	10.22	12.62	12.03	14.54

$$\begin{bmatrix} 0 & (\bar{\nabla}_P f)^T \\ \bar{\nabla}_P f & \bar{C}^{-1} \end{bmatrix} \cdot \begin{bmatrix} \lambda \\ \bar{\Delta P} \end{bmatrix} = \begin{bmatrix} f_c - f(0) \\ 0 \end{bmatrix} \quad (6)$$

The value $\bar{\Delta P}$ thus found is the most probable combination of parameters that cause an end buffer impact force equal to f_c . This value of $\bar{\Delta P}$ is known in the theory of first order reliability methods (FORM) as a *design point* (Ang 1990).

Probability of exceedance

FORM provides another important result. The *reliability index* β is defined by

$$\beta = \sqrt{\bar{\Delta P}^T \cdot \bar{C}^{-1} \cdot \bar{\Delta P}} \quad (7)$$

It can then be shown that the probability that the end buffer impact force exceeds f_c is equal to:

$$p(f > f_c) = \Phi(-\beta) \quad (8)$$

where:

Φ is the Gaussian cumulative distribution.

Results of the constraint optimisation technique

The solution of the constrained optimisation problem for various levels of reliability is presented in Tables 6 and 7 for the “Power-Off” and “Power-On” conditions respectively.

Table 7 Estimated maximum end buffer impact force from the second impact response

	Hoist Load Bottom "Power-Off"	Hoist Load Bottom "Power-On"	Hoist Load Top "Power-Off"	Hoist Load Top "Power-On"
Estimated maximum end buffer impact force for $\beta = 1$	1.96	1.51	9.11	9.95
Estimated maximum end buffer impact force for $\beta = 2$	-0.57	-1.59	11.35	11.85
Estimated maximum end buffer impact force for $\beta = 3$	-2.98	-4.69	13.58	13.75

The maximum end buffer impact force of 14.54 kN occurred for the condition "Hoist load top with Power-On" for the particular crane and crane supporting structure investigated, for a reliability index of $\beta = 3$.

The probability of exceedance is related to the reliability indices calculated using Equation 9 and is given for various reliability indices in Table 8:

$$P = \Phi(-\beta) \quad (9)$$

Figure 4 presents a comparison of the various codified impact forces with the maximum estimated end buffer impact force for $\beta = 1, 2$ and 3 . From Figure 4 it can be concluded that SABS 0160 underestimates the end buffer impact force by 18%, while SANS 10160-6 overestimates it by 64% for a target reliability index of $\beta = 3$.

It can also be concluded that SABS 0160 corresponds to $\beta = 2$. The code therefore yields an impact force which has a probability of 2.3×10^{-2} (2.3%) of being exceeded.

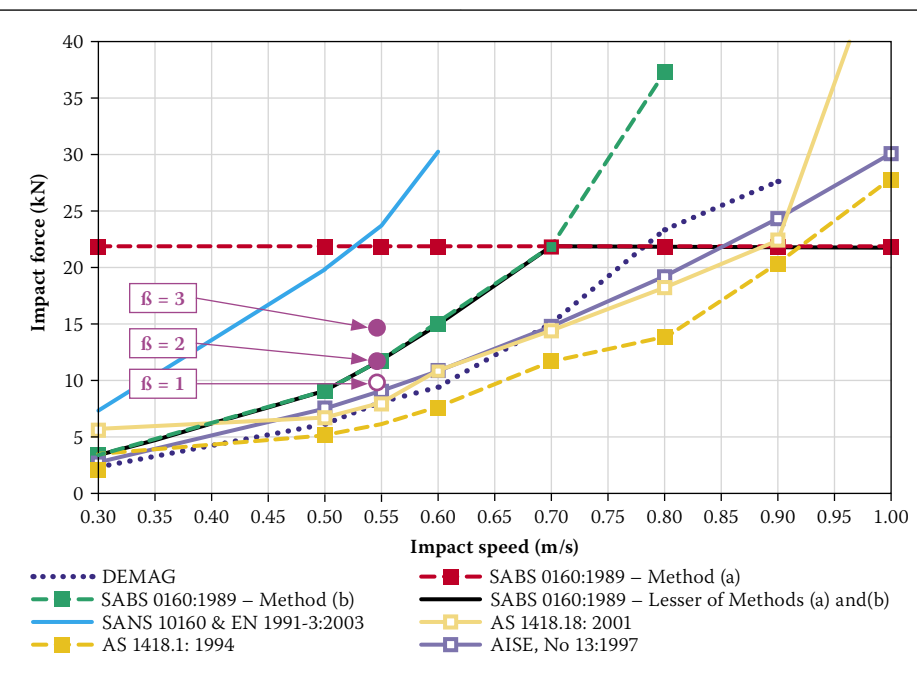
CONCLUSIONS

End buffer impact forces are the result of complex behaviour of the structure during an impact, and this behaviour is influenced by a series of parameters. Failure to adequately address these effects can lead to a catastrophe. An estimation of existing forces shows that, except for EN 1991:3 and SANS 10160-6, all other design codes result in a reliability index (β) lower than 3 as calculated in this paper using constraint optimisation. It is generally accepted that a reliability index of 3 should be used for design purposes. Thus the design codes that yield estimates lower than 3 do not meet international standards.

At this stage it is not possible to make a general recommendation as to the most important parameters, as only one impact velocity was considered. However, the present work clearly highlights the need for a revision of the code requirements. This would require the FE simulations

Table 8 Level of probability for various levels of reliability

β	Probability (%)
1	1.6×10^{-1}
2	2.3×10^{-2}
3	1.4×10^{-3}

**Figure 4** Comparison of the codified impact forces with the maximum end buffer impact force obtained from the constraint optimisation problem

to be repeated for various impact velocities, different masses and different crane configurations.

BIBLIOGRAPHY

ABAQUS. Personal communication and www.abaqus.com

Ang, H S & Tang, W H 1990. *Probability Concepts in Engineering Planning and Design, Vol. 2 – Decision, Risk, and Reliability*. New York: Wiley.

Association of Steel and Iron Engineers (AISE) 2000. *Specification for electric overhead travelling cranes for steel mill service*. Technical Report 6, Clause 3.8, pp 48–49.

DEMAG. Personal communication and www.demag.com

European Committee for Standardisation 1991. EN 1991-3:2003, *EUROCODE 1 – Actions on structures, Part 3: Actions induced by cranes and machinery*. CEN/TC250/SC1, Clause 2.11.1, pp 1–44.

Haas, T N 2007. *Numerical (FEA) evaluation of crane end buffer impact force*. PhD thesis, Department of Civil Engineering, Structural Division, Stellenbosch University.

Larson, R, Hostetler, R & Edwards, B 1995. *Calculus, Early Transcendental Functions*, 1st edition. Lexington, Mass, US: D.C. Heath and Co, pp 914–919.

Montgomery, D & Runger, G 2002. *Applied Statistics and Probability for Engineers*, 3rd edition. New York: Wiley, pp 109–112.

South African Bureau of Standards. 1989. SABS 0160-1989 (as amended 1990): *Code of Practice: the general procedure and loadings to be applied in the design of buildings*. Clauses 5.7.6 and 5.7.7, pp 95–100.

South African Bureau of Standards. SANS 10160-6: Working document on SANS 10160-6: *Basis of structural design and actions for buildings and industrial structures. Section 10: Action induced by cranes and machinery*. Personal communication with a member of the Working Group, Clause 10.2.12.1, pp 1–26.

Standards Australia. 1994. AS 1418.1:1994: *Cranes (including hoists and winches). Part 1: General requirements*, 3rd edition. Clause 4.7.5, pp 24–26.

Standards Australia. 2001. AS 1418.18:2001, *Cranes (including hoists and winches). Part 18: Crane runways and monorails*. Appendix B, p 41.